iScience

CellPress
OPEN ACCESS

Article

The fragile X locus is prone to spontaneous DNA damage that is preferentially repaired by nonhomologous end-joining to preserve genome integrity

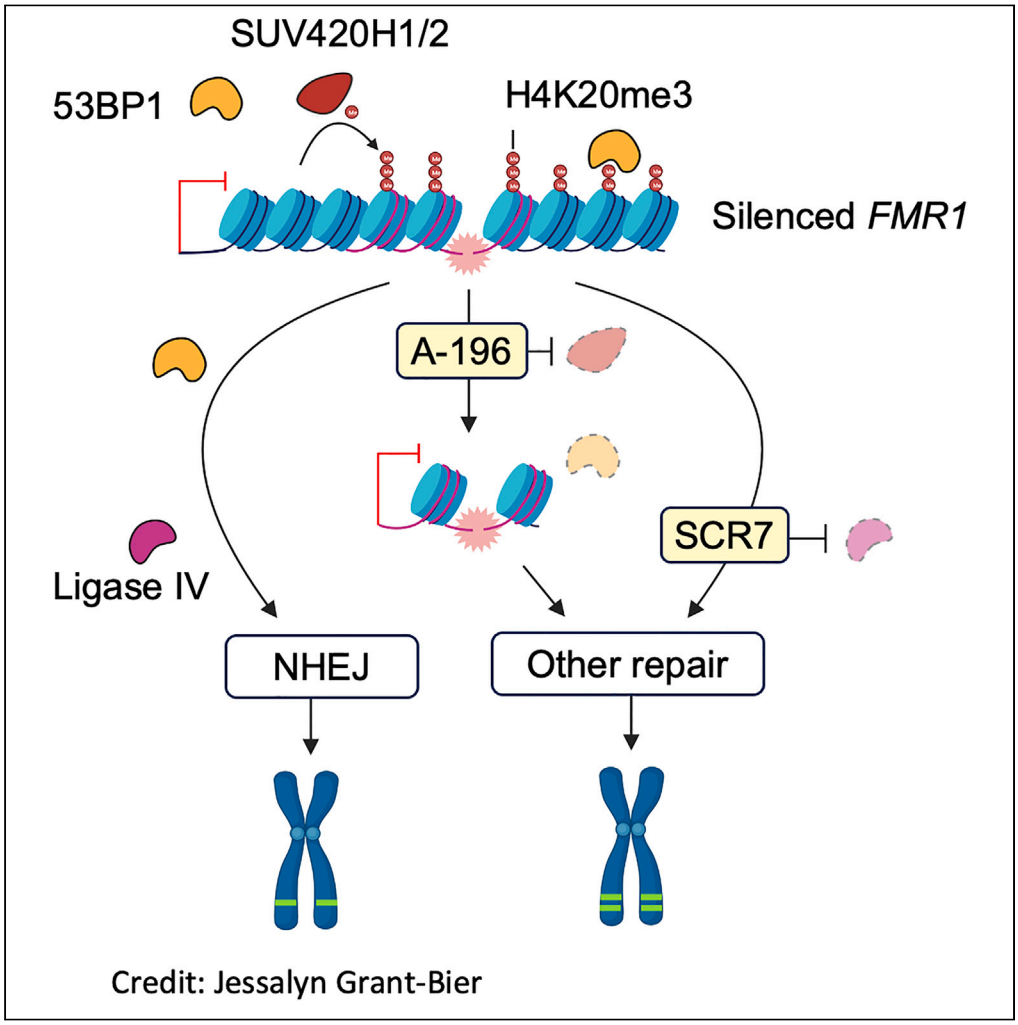

Daman Kumari, Rachel Adihe Lokanga, Cai McCann, Thomas Ried, Karen Usdin

karenu@nih.gov

Highlights

Reducing H4K20me3 does not affect *FMR1* transcription in fragile X patient cells

Reducing H4K20me2/3 increases duplications in the vicinity of fragile X locus

Reducing NHEJ using the Ligase IV inhibitor, SCR7, also increases duplications

Fragile X locus is prone to spontaneous DNA damage that is repaired by NHEJ

Kumari et al., iScience *27*, 108814
February 16, 2024
https://doi.org/10.1016/j.isci.2024.108814

iScience

CellPress
OPEN ACCESS

Article

The fragile X locus is prone to spontaneous DNA damage that is preferentially repaired by nonhomologous end-joining to preserve genome integrity

Daman Kumari,[1,4] Rachel Adihe Lokanga,[2,3,4] Cai McCann,[1] Thomas Ried,[2] and Karen Usdin[1,5,*]

SUMMARY

A long CGG-repeat tract in the *FMR1* gene induces the epigenetic silencing that causes fragile X syndrome (FXS). Epigenetic changes include H4K20 trimethylation, a heterochromatic modification frequently implicated in transcriptional silencing. Here, we report that treatment with A-196, an inhibitor of SUV420H1/H2, the enzymes responsible for H4K20 di-/trimethylation, does not affect *FMR1* transcription, but does result in increased chromosomal duplications. Increased duplications were also seen in FXS cells treated with SCR7, an inhibitor of Lig4, a ligase essential for NHEJ. Our study suggests that the fragile X (FX) locus is prone to spontaneous DNA damage that is normally repaired by NHEJ. We suggest that heterochromatinization of the FX allele may be triggered, at least in part, in response to this DNA damage.

INTRODUCTION

Repeat expansion diseases (REDs) are caused by an increase in the number of repeat units in a single, disease-specific short tandem repeat (STR) array or microsatellite.[1] In a subset of these diseases, the expansions induce heterochromatin formation and gene silencing via a process that is not fully understood. In the case of fragile X syndrome (FXS), the most common monogenic cause of intellectual disability and autism, the repeat responsible is a CGG repeat tract located in the 5′ UTR of the X-linked Fragile X Messenger Ribonucleoprotein 1 (*FMR1*) gene. *FMR1* encodes Fragile X Messenger Ribonucleoprotein 1 Protein (FMRP), a protein important for translational regulation.[2] The CGG repeat number is polymorphic in general population and typical alleles have <55 CGG repeats. Alleles with 55–200 CGGs are referred to as premutation (PM) alleles while alleles with >200 CGGs are referred to as full mutations (FM) (Figure 1A). PM alleles are prone to gain repeats both in the germline and soma with PM alleles expanding into the FM range when passed through the female germ line. However, the exact timing and the mechanism of repeat expansion is not fully understood.[3,4] PM alleles are hyper-expressed[5] and associated with two different disorders, fragile X-associated tremor/ataxia syndrome (FXTAS) and fragile X-associated primary ovarian insufficiency (FXPOI).[6] In contrast, FM alleles accumulate epigenetic modifications characteristic of heterochromatin. These modifications include DNA methylation, hypoacetylated H3 and H4 histones, histone H3 dimethylated and trimethylated at lysine 9 (H3K9me2 and H3K9me3 respectively) and trimethylated at lysine 27 (H3K27me3), and histone H4 trimethylated at lysine 20 (H4K20me3).[7–11] The net result is that the transcription of these alleles is substantially reduced or eliminated. This results in a deficiency of FMRP which causes FXS. These alleles are also associated with an eponymous fragile site that is seen when cells are grown under folate-stress.[12] This fragile site is thought to result from stalled replication forks associated with long CGG-repeat tracts.[13] These stalled forks necessitate the use of an error-prone form of double-strand break repair (DSBR) known as break-induced replication (BIR) in order to rescue the collapsed fork.[14–16] While it is thought that FM alleles are silenced sometime during early embryonic development, the exact timing is not known,[17] partly due to the lack of a suitable animal model that recapitulates repeat-mediated *FMR1* gene silencing. Furthermore, how, and why FM alleles, but not PM alleles, trigger this gene silencing is unknown.

We and others have previously demonstrated that epigenetic changes are also associated with the GAA-expansion in the frataxin (*FXN*) gene that causes Friedreich's ataxia (FRDA), another RED.[18–20] These epigenetic changes also include elevated levels of H4K20me3.[20] Recent work has shown that treatment of FRDA patient cells with A-196, a nontoxic, potent and selective inhibitor of SUV420H1 and SUV420H2, the histone methyltransferases responsible for di- and trimethylation of H4K20,[21] resulted in a 2-fold increase in *FXN* transcription.[22] This would be consistent with a role for one or both chromatin marks in repeat-mediated gene silencing in FRDA. To assess whether inhibition of H4K20

[1]Section on Gene Structure and Disease, Laboratory of Cell and Molecular Biology, National Institute of Diabetes, Digestive and Kidney Diseases, National Institutes of Health, Bethesda, MD 20892, USA
[2]Section of Cancer Genomics, Center for Cancer Research, National Cancer Institute, National Institutes of Health, Bethesda, MD 20892, USA
[3]Present address: Division of Biotechnology Review and Research III, Office of Biotechnology Products, Office of Pharmaceutical Quality, Center for Drug Evaluation and Research, U.S. Food and Drug Administration, Silver Spring, MD 20993
[4]These authors contributed equally
[5]Lead contact
*Correspondence: karenu@nih.gov
https://doi.org/10.1016/j.isci.2024.108814

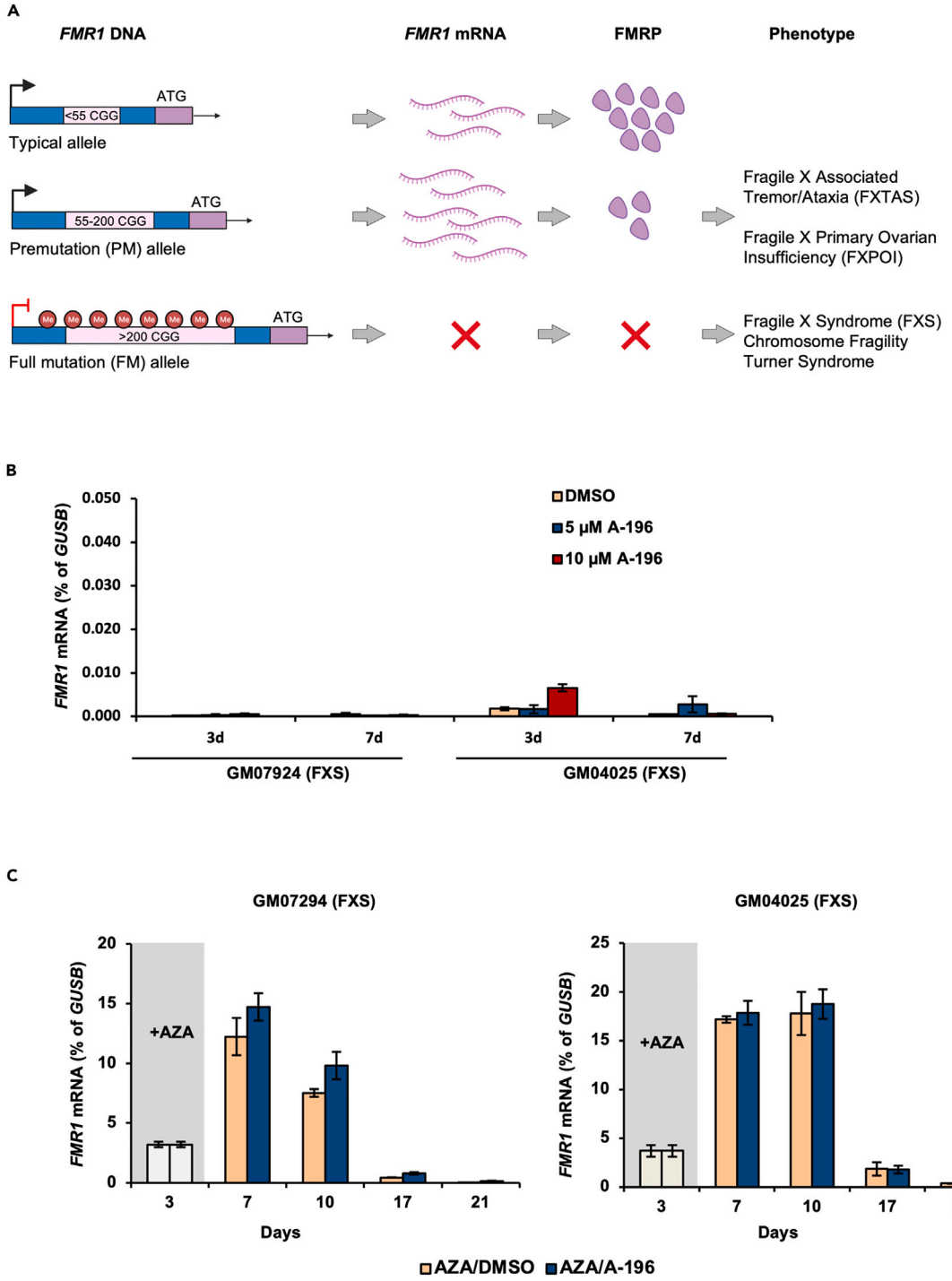

Figure 1. A-196 treatment does not affect *FMR1* expression

(A) Schematic showing different *FMR1* alleles seen in the human population.

(B) FXS cells were treated with DMSO, 5 µM A-196 or 10 µM A-196 for 3 days and 7 days and collected for RNA isolation.

(C) FXS cells were treated with 10 µM AZA for 3 days and then the medium was changed to either with DMSO or 5 µM A-196. Samples were collected for RNA isolation at indicated time. The levels of *FMR1* and *GUSB* mRNA were measured by RT-qPCR. *FMR1* mRNA levels are shown as a percentage of *GUSB* mRNA. The data shown are an average from two independent treatments and the error bars represent standard deviation.

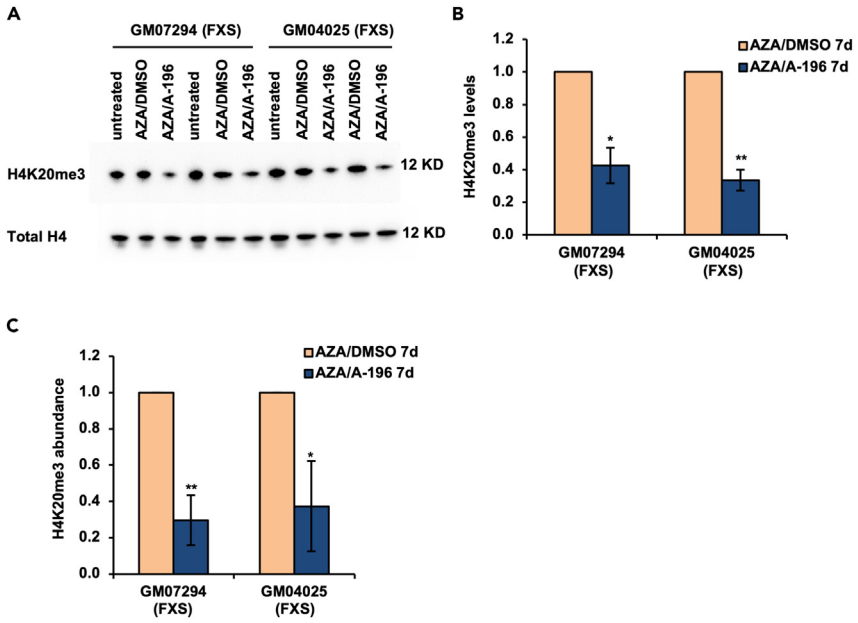

Figure 2. A-196 treatment decreases H4K20me3

(A–C) FXS cells were treated with 10 μM AZA for 3 days and then the medium was changed to either with DMSO or 5 μM A-196. The cells were grown for another 4 days and then processed for lysate preparation for western blotting and chromatin preparation for ChIP assay. (A) A representative Western blot is shown. (B) Quantitation for H4K20me3 levels from three independent western blots. The levels of H4K20me3 were normalized to the levels of total H4 and are shown relative to AZA/DMSO. The error bars represent standard deviation. The two-tailed p value was calculated using paired t-test, *p = 0.012, **p = 0.0031. (C) ChIP assay was done with an antibody to H4K20me3. The % input data for *FMR1* exon1 region were calculated and normalized to AZA/DMSO. Data shown are an average from 3 independent treatments. Error bars represent standard deviation. Two-tailed p value was calculated using the paired t-test, *p = 0.048, **p = 0.01.

di-/trimethylation would have a similar effect on *FMR1* gene expression in FXS patient cells, we treated them with A-196. Our data suggest that H4K20 trimethylation does not contribute to transcription silencing of the *FMR1* gene in FXS. However, reducing the levels of H4K20 di-/trimethylation with A-196 revealed a high level of spontaneous DNA damage at the *FMR1* locus that is preferentially repaired by nonhomologous end-joining (NHEJ) to preserve genome integrity.

RESULTS

H4K20 di/trimethylation is not required for the maintenance of *FMR1* gene silencing

To assess the role of H4K20me3 in *FMR1* gene silencing, we treated two different FXS patient lymphoblastoid cell lines with vehicle (DMSO) alone or with different concentrations of the SUV420H1/H2 inhibitor, A-196. We then analyzed the levels of *FMR1* mRNA with RT-qPCR using *GUSB* as a normalizing control. At concentrations below 12.5 μM, A-196 no effect is seen on the viability or the growth rate of multiple cell types.[21] No appreciable *FMR1* mRNA was detected after treatment with 5 μM or 10μM A-196 for 3 or 7 days (Figure 1B). In contrast, typical alleles produce *FMR1* mRNA levels similar to *GUSB*.[23] This suggests that inhibition of H4K20me3 alone does not result in *FMR1* gene reactivation. This is similar to what we had previously observed when H3K27 trimethylation and H3K9 dimethylation were inhibited.[23,24] However, when cells are pretreated with the DNA methyltransferase inhibitor, 5-azadeoxycytidine (AZA), to remove DNA methylation and reactivate the gene, inhibition of H3K27 trimethylation or H3K9 dimethylation delays re-silencing.[23,24] This is consistent with the idea that these histone modifications are important for *FMR1* gene silencing. To test whether the same was true of H4K20me3, we reactivated the *FMR1* gene by treatment with AZA for 3 days as we had done previously, and then treated cells with either DMSO or 5 μM A-196 for 21 days, adding fresh drug every 7 days. However, in contrast to what was previously seen with the inhibitors of H3K27 or H3K9 methylation, the *FMR1* gene was completely re-silenced by day 21 in cells treated with A-196 (Figure 1C).

To verify the efficacy of the A-196 treatments, we analyzed the changes in global levels of H4K20me3 after treatment with AZA and A-196 at day 7 by western blotting and on the *FMR1* gene specifically by chromatin immunoprecipitation (ChIP). We observed a significant decrease in the global levels of H4K20me3 after A-196 treatment (Figures 2A and 2B). Moreover, the levels of H4K20me3 were also significantly reduced at the *FMR1* gene (Figure 2C). Thus, our data demonstrate that a decrease in H4K20me3 levels does not affect the transcriptional activity of FM alleles even when the gene is demethylated.

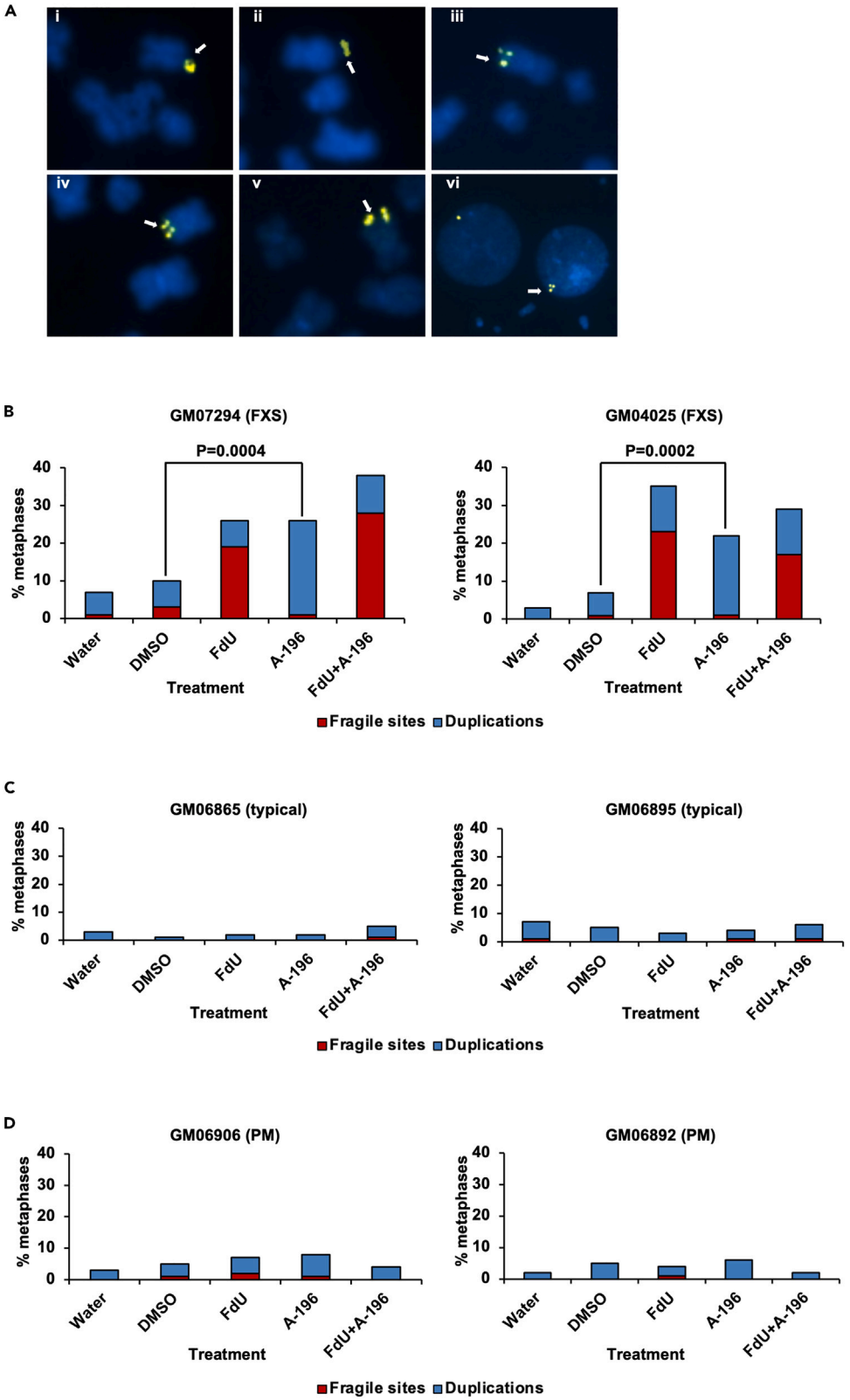
A
i
ii
iii
iv
v
vi
B
GM07294 (FXS)
P=0.0004
GM04025 (FXS)
P=0.0002
% metaphases
0
10
20
30
40
Water
DMSO
FdU
A-196
FdU+A-196
Treatment
Fragile sites
Duplications
C
GM06865 (typical)
GM06895 (typical)
D
GM06906 (PM)
GM06892 (PM)

Figure 3. A-196 treatment causes an increase in chromosomal duplications at the FX locus

(A) Representative metaphases seen in FXS lymphoblastoid cells after treatment with 0.1 μM FdU and/or 5 μM A-196. (i) FISH image showing X chromosome with breakage of one sister chromatid and loss of the FRAXA region on the other. (ii) X chromosome showing breakage of both sister chromatids. (iii) FISH showing X chromosome in which one chromatid shows what appears to be a partial duplication of part of the FRAXA region. (iv, v) X chromosome in which both sister chromatids show duplication of the FRAXA region. (vi) Example of duplication of the FRAXA region seen in interphase nucleus.

(B–D) Percentage of metaphases showing fragile sites and duplications after treatment of FXS (B), typical (C) and premutation (D) cell lines with 0.1 μM FdU for 18 h and with DMSO or 5 μM A-196 for 3 days. For A-196 + FdU treatment, cells were treated with 5 μM A-196 for 3 days and 0.1 μM FdU was added for the last 18h of the treatment. Two-tailed p value was calculated using Fisher's exact test using the actual number of metaphases showing duplications and/or fragile sites. No significant difference was seen in the percentage of metaphases showing fragile sites and duplications after treatment with A-196 in typical and premutation cells. See also Table S1.

A-196 causes an increase in chromosomal duplications at the FX locus

Normal *FMR1* alleles replicate late in the cell cycle,[25] with silenced FM alleles replicating even later.[26,27] Since H4K20me3 has been implicated in the activation of a subset of late replication origins,[28] we wondered whether A-196 treatment might result in a further delay in completion of replication of this region by preventing the use of such origins. If so, FXS cells might enter mitosis with the *FMR1* locus still not fully replicated. This could result in the initiation of mitotic DNA synthesis (MiDAS) analogous to what is seen when replication is slowed by fluoro-2′-deoxyuridine (FdU). FdU treatment is associated with chromosome fragility, a break/gap on the chromosome that is visible in metaphase (FRAXA fragile site) that is thought to reflect *FMR1* alleles that have not yet completed replication.[29,30] We thus tested the effect of A-196 on expression of the FRAXA fragile site using a bacterial artificial chromosome (BAC) 1.5 MB telomeric to *FMR1* as a fluorescence *in situ* hybridization (FISH) probe. Representative examples of chromosomal abnormalities seen in response to FdU and A-196 are shown in Figure 3A. As can be seen in Figure 3B, A-196 treatment caused no increase in chromosome fragility relative to DMSO in FXS patient cell lines. Since fragility is a hallmark of FX chromosomes that have not yet completed replication when the cell enters metaphase, our data suggests that A-196 does not significantly delay replication. No significant change in the frequency of fragile sites was seen when cells were treated with both A-196 and FdU relative to FdU alone (two-tailed p value = 0.1275 for GM07294 and 0.39 for GM04025 using the Fisher's exact test, Figure 3B).

While there was no increase in the frequency of chromosome fragility after A-196 treatment, we did see a significant increase in duplications of the FISH signal on the long arm of the X chromosome (Figure 3B). MiDAS in response to FdU is thought to occur via BIR, a homology driven DNA repair process that is also associated with an increase in chromosome duplications.[31,32] Thus, while A-196 treated cells do not seem to require MiDAS, it is possible that they are using a similar repair process that is complete before mitosis begins. Cells treated with both FdU and A-196 also showed a trend toward a decrease in the number of duplications but this did not reach statistical significance (two-tailed p value = 0.09 for GM07294 and 0.24 for GM04025 using the Fisher's exact test, Figure 3B). The decrease in the frequency of duplications may reflect FdU's effect on slowing replication. This would result in a delay in the completion of downstream events in BIR that would lead to duplications.

To test whether duplications were also seen in cells with typical or PM alleles, we tested two cell lines with typical *FMR1* allele sizes and two cell lines with PM alleles. A-196 treatment did not result in an increase in duplications in any of these lines (Figures 3C and 3D). Thus, the effect of A-196 on increasing the number of duplications was specific to FM alleles.

H4K20 di- and trimethylation is associated with 53BP1 recruitment.[33–35] 53BP1 in turn blocks the 3′ end resection that would be required for homology driven repair pathways like BIR, thus favoring the use of NHEJ.[35] A-196 treatment also decreased the levels of both H4K20me2 (Figure 4A) and 53BP1 levels (Figure 4B) on FM alleles which would likely shift repair toward a homology driven pathway. While we had previously shown that typical and PM alleles showed no enrichment of H4K20me3, the levels of H4K20me2 were similar on typical, PM and FM alleles (Figure S1A). The levels of 53BP1 on typical and PM alleles were slightly lower than they were on FM alleles, although this difference did not reach statistical significance (Figure S1B). However, it should be noted that because of the effect of repeat length on the efficiency of PCR, the levels of these proteins were measured in the region adjacent to the repeat, leaving open the possibility that more significant differences in 53BP1 levels would be seen on the repeat itself.

Inhibition of Lig4 also increases duplications in FXS patient cells

We also treated FXS cells with SCR7,[36] a small molecule inhibitor of Lig4, a ligase required for NHEJ and examined the *FMR1* FISH signal on metaphase spreads. There was no significant increase in the number of fragile sites seen with SCR7 treatment (Figure 4C; Table S1). However, the number of duplications was significantly higher than those seen in DMSO treated cells (two-tailed p value by Fisher's exact test = 0.0039 for GM07294 and 0.0043 for GM04025 cells) and comparable to the number of duplications observed with A-196 (Figure 4C). No increase in duplications was seen with SCR7 treatment in typical or PM cells (Table S1). These observations are consistent with the idea that FM alleles are prone to spontaneous DNA damage that can be repaired via NHEJ.

To test for a role of homologous recombination pathways in repair of this damage, we then analyzed the frequency of chromosomal abnormalities in cells treated with B02, a small molecule inhibitor of RAD51, an important HR protein.[37] We used a B02 concentration of 10 μM for our experiments, a concentration shown to significantly reduce HR in multiple cell types.[38,39] B02 treatment of FXS cells showed a duplication frequency that was intermediate between that seen in the DMSO and SCR7 treated cells. However, the differences were not statistically significant (two-tailed p value by Fisher's exact test = 0.103 for GM04025 and 0.159 for GM07294, Table S1). No increase in duplications was seen in typical and PM cells (Table S1).

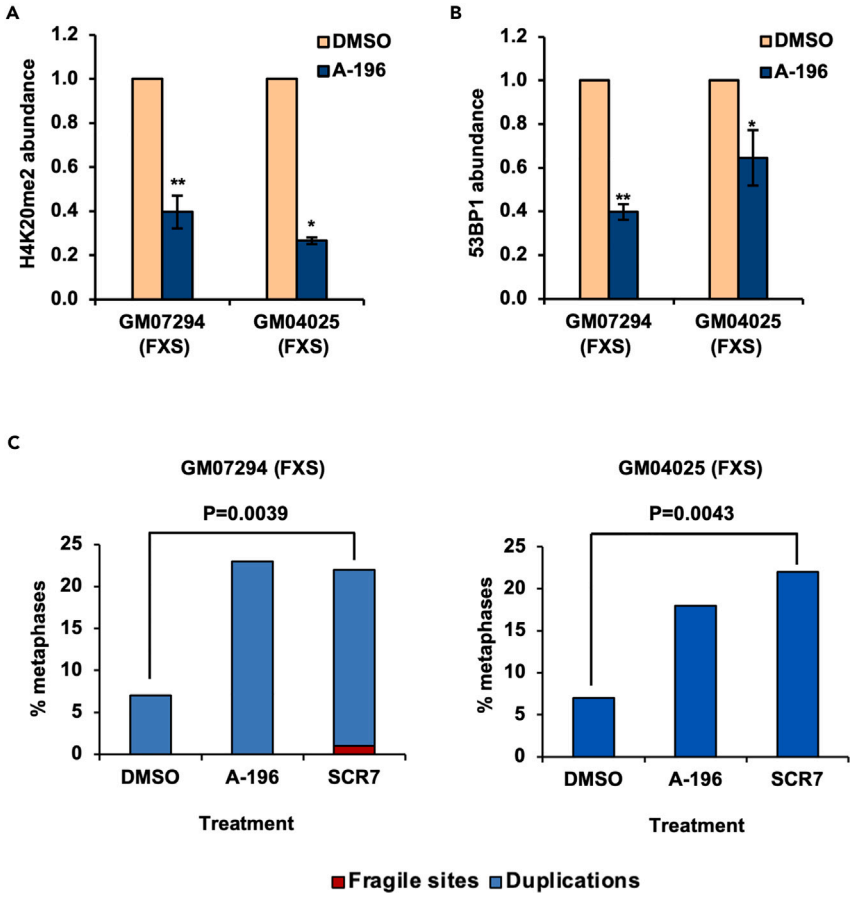

Figure 4. Inhibition of nonhomologous end-joining is responsible for chromosomal duplications seen at the FX locus

(A) FXS cells were treated with DMSO and 5 μM A-196 for 3 days and ChIP was done using an antibody to H4K20me2. The abundance of H4K20me2 at the *FMR1* exon 1 was calculated as % input and is shown relative to DMSO. Data shown are an average from 3 independent experiments for GM07294 and 2 independent experiments for GM04025. Error bars represent standard deviation, two-tailed p value was calculated by paired t-test, *p = 0.009. **p = 0.005.

(B) FXS cells were treated with DMSO and 5 μM A-196 for 3 days and ChIP was done using an antibody to 53BP1. The abundance of 53BP1 at the *FMR1* exon 1 was calculated as % input and is shown relative to DMSO. Data shown are an average from 3 independent ChIP experiments. Error bars represent standard deviation, two-tailed p value was calculated by paired t-test, *p = 0.039. **p = 0.001.

(C) Percentage of metaphases showing fragile sites and duplications in FXS cells after treatment with 5 μM A-196 or 10 μM SCR7 for 3 days. Two-tailed p value was calculated using Fisher's exact test using the actual number of metaphases showing duplications and/or fragile sites. See also Figure S1 and Table S1.

DISCUSSION

The H4K20me3 mark is enriched at pericentric heterochromatin in mammals where it contributes to transcription silencing.[40] However, we show here that while this histone modification is also enriched on the heterochromatin associated with silenced *FMR1* (FM) alleles, it is not required for transcriptional silencing at this locus. Rather, depletion of di- and trimethylation marks on FM alleles with A-196 resulted in an increase in chromosome duplications. A similar result was seen for cells grown in the presence of a Lig4 inhibitor. This would be consistent with the idea that FM alleles are prone to DNA damage even under normal growth conditions and that H4K20me2/me3 plays a role in ensuring that this damage is repaired by NHEJ, rather than a homology-driven repair process that produces a high frequency of chromosomal abnormalities. The damage may be a consequence of the propensity of long CGG-repeat tracts to cause DNA polymerase stalling.[13,41–50] The error-prone process that gives rise to duplications may resemble the events associated with the MiDAS that is thought to occur at the FX locus in response to replication stalling associated with FdU treatment.[29,31] This MiDAS involves a form of BIR.[29,31] We speculate that the occasional failure of NHEJ to repair the damage results in error-prone repair that contributes to the high frequency of mosaicism for repeat number seen in FM carriers.[51] It may also account for the high frequency loss of the affected X chromosome that is seen in female FX fetuses[52] and the frequent deletions or duplications associated with FM alleles.[53–56] Interestingly, in some cases these events are associated with a sequence signature characteristic of microhomology mediated BIR.[54]

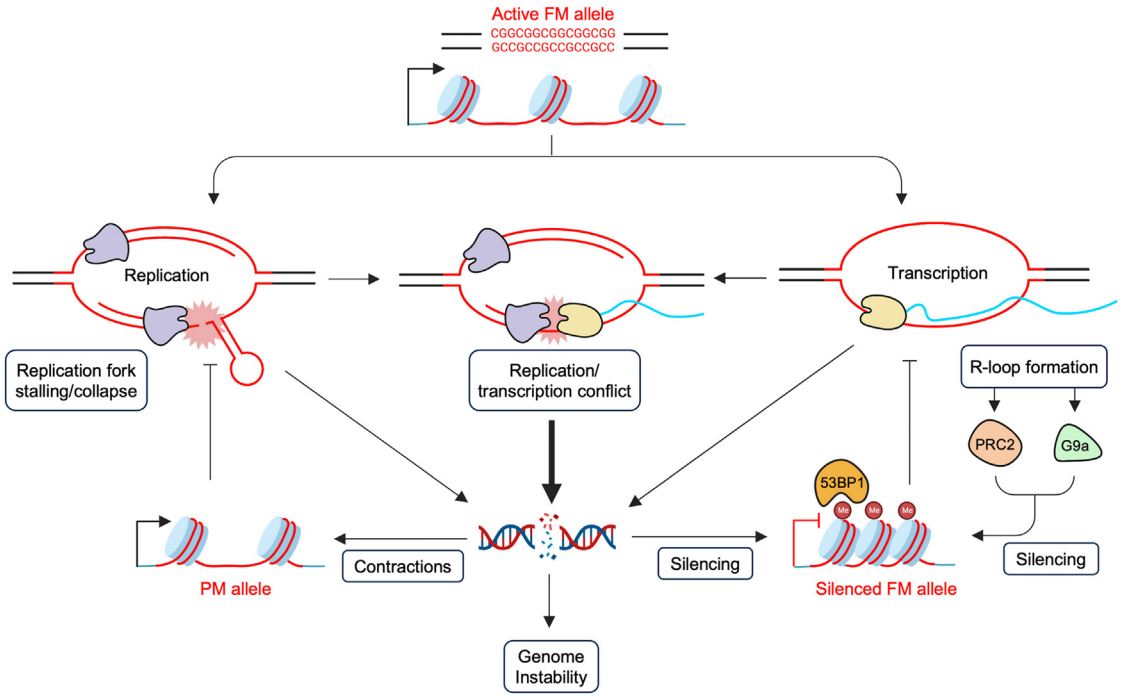

Figure 5. Model for CGG repeat expansion induced *FMR1* gene silencing

Expansion of CGG repeats leads to increased replication stalling/fork collapse due to the formation of secondary structures that block fork progression.[13,41] This problem is further exacerbated by replication-transcription conflicts in cells carrying active FM alleles. Stalled replication forks could lead to increased genomic instability including chromosome fragility and repeat contraction. Contraction of the repeats would reduce the likelihood of replication fork stalling to some degree. The stable R-loop associated with transcription of the FM alleles would facilitate recruitment of G9a and PRC2 leading to gene silencing, which in turn would reduce the risk further by reducing replication-transcription conflicts. While silencing would reduce replication-transcription conflicts, residual fork stalling could still threaten genome integrity. Recruitment of H3K9me3 and H4K20me3 may mitigate this danger by facilitating NHEJ in part by maximizing 53BP1 binding.

It may be that chronic DNA damage at FM alleles, perhaps resulting from a persistent replication fork block formed by the repeat, results in recruitment of H4K20me3, a view consistent with our previous observations that unlike H3K9me2 and H3K27me3 which are widely distributed across the 5′ end of the *FMR1* gene, H4K20me3 is concentrated in the region containing the repeat.[9] We hypothesize that rather than playing a role in transcriptional silencing, this modification represents one way that cells respond to the threat to genomic integrity presented by the expanded repeat.

Our findings suggest that while H4K20me3 levels are higher on the region flanking the repeat of FM alleles than typical or PM alleles, 53BP1 is only modestly increased, although a higher level of enrichment on the repeat itself cannot be excluded. It may be that the 53BP1 enrichment on all allele size classes reflects the problems associated with replication of CGG-repeat tracts even the relatively short ones found on normal alleles.[50] This replication stress might be exacerbated in the case of active alleles, by the formation of stable R-loops and the increased risk of transcription-replication collisions (TRCs).[23,57,58] We speculate that the relatively modest reduction of 53BP1 associated with A-196 treatment still leaves enough residual protein to facilitate any repair needed at typical and PM alleles but is not sufficient to neutralize the effect of the larger and more damaging FM alleles. H4K20me3 may represent an additional layer of protection present on FM alleles that reduces the incidence of genome instability, perhaps via its interaction with H3K9me3, a histone modification we have shown to colocalize with H4K20me3 on the repeat tract,[9] that has been proposed to act in concert with H4K20me3 in the response to DNA damage.[35] Nonetheless, our SCR7 data suggest that FM alleles are prone to a high levels of DNA damage under normal growth conditions and that NHEJ repairs the damage, thus reducing the threat to genome integrity posed by FM alleles.

A number of studies suggest a link between replication stress and heterochromatin formation (reviewed in[59]) and support a model where prolonged replication pausing would increase the probability of heterochromatin formation.[60] It may be that transcriptional silencing of FM alleles is one way for the cell to limit DNA damage and protect genome integrity when other protective mechanisms are no longer sufficient as illustrated in Figure 5. In the absence of transcriptional silencing, repeat contraction may be an alternate mechanism to limit replication stress. This hypothesis is supported by the observation that unmethylated FM alleles show an elevated level of contractions,[61–64] a process that has been shown to be related to R-loop formation.[61]

We have previously reported a high frequency of duplications in Friedreich's ataxia (FRDA) patient cells.[65] FRDA is caused by an expanded GAA/TTC tract in intron 1 of the frataxin (*FXN*) gene. Long GAA/TTC tracts also cause replication fork stalling.[50,66] The fact that enrichment for H4K20me3 is also seen on such alleles,[20] raises the possibility that in addition to contributing to gene silencing in FRDA,[22] this modification

may also act to protect genome integrity at this locus, as well as, perhaps, the loci associated with other repeat expansion diseases that are caused by repeats that stall DNA synthesis.

Limitations of the study

This study used A-196, a small molecule inhibitor of both SUV420H1 and SUV420H2, to examine the effect of H4K20me2 and H4K20me3 at the fragile X locus. This revealed high levels of spontaneous DNA damage at the *FMR1* locus in FX patient cells, although the use of A-196 doesn't allow us to specifically attribute a role of H4K20me3 in this process. However, specific knockdown of SUV420H2 is difficult to accomplish in lymphoblastoid cells due to the low efficiency of nucleic acid delivery in this cell type, coupled with the difficulties associated with isolation of clonal cell lines that complicate CRISPR knockout approaches. Whatever the role of H4K20me3 in this process, our data clearly show that this histone modification is not directly involved in the silencing of FM alleles and that FM alleles are prone to high levels of spontaneous DNA damage. While the FISH studies did allow us to identify chromosomal duplications associated with FM alleles, this approach does not allow us to examine the full spectrum of changes that might arise at this locus. In principle, long read sequencing could allow such changes to be identified. However, given the heterogeneity of the likely products and the limited read depth, this approach is currently challenging and any PCR enrichment to increase the number of relevant reads would be prone to bias because of the difficulties amplifying long CGG-repeat tracts.[41] Nonetheless, while a full description of the mutational spectrum generated by long CGG-repeats awaits technological improvements, our data provide clear evidence that the long CGG-repeats present in FM alleles provide a continuous threat to genome integrity that may help shape its chromatin landscape.

STAR★METHODS

Detailed methods are provided in the online version of this paper and include the following:

- KEY RESOURCES TABLE
- RESOURCE AVAILABILITY
  - Lead contact
  - Materials availability
  - Data and code availability
- EXPERIMENTAL MODEL AND STUDY PARTICIPANT DETAILS
  - Human cell lines
- METHOD DETAILS
  - Cell culture and drug treatments
  - RNA methods
  - Western blotting
  - Chromatin immunoprecipitation
  - Fluorescent *in situ* hybridization (FISH)
- QUANTIFICATION AND STATISTICAL ANALYSIS

SUPPLEMENTAL INFORMATION

Supplemental information can be found online at https://doi.org/10.1016/j.isci.2024.108814.

ACKNOWLEDGMENTS

We want to thank members of the Usdin lab and Dr Mirit Aladjem (NCI) for their careful reading of the manuscript and helpful comments. We thank Jessalyn Grant-Bier for drawing the graphical abstract, Figures 1A and 5 which were generated using Biorender.com. This work was supported by the National Institutes of Health [DK057808 to K.U.]. Funding for open access charge: National Institutes of Health.

AUTHOR CONTRIBUTIONS

Conceptualization, D.K. and K.U.; methodology, D.K., R.L., and K.U.; investigation, D.K., R.L., and C.M.; data interpretation, D.K., R.L., and K.U.; writing-original draft, D.K. and K.U.; writing–review and editing, all authors; funding acquisition, K.U.; resources, K.U. and T.R.; supervision, K.U.

DECLARATION OF INTERESTS

The authors declare no competing interests.

Received: September 8, 2023
Revised: October 26, 2023
Accepted: January 2, 2024
Published: January 6, 2024

REFERENCES

1. Paulson, H. (2018). Repeat expansion diseases. Handb. Clin. Neurol. *147*, 105–123.
2. Darnell, J.C., Van Driesche, S.J., Zhang, C., Hung, K.Y.S., Mele, A., Fraser, C.E., Stone, E.F., Chen, C., Fak, J.J., Chi, S.W., et al. (2011). FMRP stalls ribosomal translocation on mRNAs linked to synaptic function and autism. Cell *146*, 247–261.
3. Jin, P., and Warren, S.T. (2000). Understanding the molecular basis of fragile X syndrome. Hum. Mol. Genet. *9*, 901–908.
4. Tabolacci, E., Nobile, V., Pucci, C., and Chiurazzi, P. (2022). Mechanisms of the FMR1 Repeat Instability: How Does the CGG Sequence Expand? Int. J. Mol. Sci. *23*, 5425.
5. Tassone, F., Hagerman, R.J., Taylor, A.K., Gane, L.W., Godfrey, T.E., and Hagerman, P.J. (2000). Elevated levels of FMR1 mRNA in carrier males: a new mechanism of involvement in the fragile-X syndrome. Am. J. Hum. Genet. *66*, 6–15.
6. Hagerman, R.J., and Hagerman, P.J. (2002). The fragile X premutation: into the phenotypic fold. Curr. Opin. Genet. Dev. *12*, 278–283.
7. Biacsi, R., Kumari, D., and Usdin, K. (2008). SIRT1 inhibition alleviates gene silencing in Fragile X mental retardation syndrome. PLoS Genet. *4*, e1000017.
8. Coffee, B., Zhang, F., Warren, S.T., and Reines, D. (1999). Acetylated histones are associated with FMR1 in normal but not fragile X-syndrome cells. Nat. Genet. *22*, 98–101.
9. Kumari, D., and Usdin, K. (2010). The distribution of repressive histone modifications on silenced FMR1 alleles provides clues to the mechanism of gene silencing in fragile X syndrome. Hum. Mol. Genet. *19*, 4634–4642.
10. Oberlé, I., Rousseau, F., Heitz, D., Kretz, C., Devys, D., Hanauer, A., Boué, J., Bertheas, M.F., and Mandel, J.L. (1991). Instability of a 550-base pair DNA segment and abnormal methylation in fragile X syndrome. Science *252*, 1097–1102.
11. Pieretti, M., Zhang, F.P., Fu, Y.H., Warren, S.T., Oostra, B.A., Caskey, C.T., and Nelson, D.L. (1991). Absence of expression of the FMR-1 gene in fragile X syndrome. Cell *66*, 817–822.
12. Lubs, H.A. (1969). A marker X chromosome. Am. J. Hum. Genet. *21*, 231–244.
13. Voineagu, I., Surka, C.F., Shishkin, A.A., Krasilnikova, M.M., and Mirkin, S.M. (2009). Replisome stalling and stabilization at CGG repeats, which are responsible for chromosomal fragility. Nat. Struct. Mol. Biol. *16*, 226–228.
14. Gadgil, R.Y., Romer, E.J., Goodman, C.C., Rider, S.D., Jr., Damewood, F.J., Barthelemy, J.R., Shin-Ya, K., Hanenberg, H., and Leffak, M. (2020). Replication stress at microsatellites causes DNA double-strand breaks and break-induced replication. J. Biol. Chem. *295*, 15378–15397.
15. Minocherhomji, S., Ying, S., Bjerregaard, V.A., Bursomanno, S., Aleliunaite, A., Wu, W., Mankouri, H.W., Shen, H., Liu, Y., and Hickson, I.D. (2015). Replication stress activates DNA repair synthesis in mitosis. Nature *528*, 286–290.
16. Xu, X., Xu, Y., Guo, R., Xu, R., Fu, C., Xing, M., Sasanuma, H., Li, Q., Takata, M., Takeda, S., et al. (2021). Fanconi anemia proteins participate in a break-induced-replication-like pathway to counter replication stress. Nat. Struct. Mol. Biol. *28*, 487–500.
17. Mor-Shaked, H., and Eiges, R. (2018). Reevaluation of FMR1 Hypermethylation Timing in Fragile X Syndrome. Front. Mol. Neurosci. *11*, 31.
18. Greene, E., Mahishi, L., Entezam, A., Kumari, D., and Usdin, K. (2007). Repeat-induced epigenetic changes in intron 1 of the frataxin gene and its consequences in Friedreich ataxia. Nucleic Acids Res. *35*, 3383–3390.
19. Herman, D., Jenssen, K., Burnett, R., Soragni, E., Perlman, S.L., and Gottesfeld, J.M. (2006). Histone deacetylase inhibitors reverse gene silencing in Friedreich's ataxia. Nat. Chem. Biol. *2*, 551–558.
20. Kim, E., Napierala, M., and Dent, S.Y.R. (2011). Hyperexpansion of GAA repeats affects post-initiation steps of FXN transcription in Friedreich's ataxia. Nucleic Acids Res. *39*, 8366–8377.
21. Bromberg, K.D., Mitchell, T.R.H., Upadhyay, A.K., Jakob, C.G., Jhala, M.A., Comess, K.M., Lasko, L.M., Li, C., Tuzon, C.T., Dai, Y., et al. (2017). The SUV4-20 inhibitor A-196 verifies a role for epigenetics in genomic integrity. Nat. Chem. Biol. *13*, 317–324.
22. Vilema-Enríquez, G., Quinlan, R., Kilfeather, P., Mazzone, R., Saqlain, S., Del Molino Del Barrio, I., Donato, A., Corda, G., Li, F., Vedadi, M., et al. (2020). Inhibition of the SUV4-20 H1 histone methyltransferase increases frataxin expression in Friedreich's ataxia patient cells. J. Biol. Chem. *295*, 17973–17985.
23. Kumari, D., and Usdin, K. (2016). Sustained expression of FMR1 mRNA from reactivated fragile X syndrome alleles after treatment with small molecules that prevent trimethylation of H3K27. Hum. Mol. Genet. *25*, 3689–3698.
24. Kumari, D., Sciascia, N., and Usdin, K. (2020). Small Molecules Targeting H3K9 Methylation Prevent Silencing of Reactivated FMR1 Alleles in Fragile X Syndrome Patient Derived Cells. Genes *11*, 356.
25. Hansen, R.S., Canfield, T.K., Lamb, M.M., Gartler, S.M., and Laird, C.D. (1993). Association of fragile X syndrome with delayed replication of the FMR1 gene. Cell *73*, 1403–1409.
26. Hansen, R.S., Canfield, T.K., Fjeld, A.D., Mumm, S., Laird, C.D., and Gartler, S.M. (1997). A variable domain of delayed replication in FRAXA fragile X chromosomes: X inactivation-like spread of late replication. Proc. Natl. Acad. Sci. USA *94*, 4587–4592.
27. Webb, T. (1992). Delayed replication of Xq27 in individuals with the fragile X syndrome. Am. J. Med. Genet. *43*, 1057–1062.
28. Brustel, J., Kirstein, N., Izard, F., Grimaud, C., Prorok, P., Cayrou, C., Schotta, G., Abdelsamie, A.F., Déjardin, J., Méchali, M., et al. (2017). Histone H4K20 tri-methylation at late-firing origins ensures timely heterochromatin replication. EMBO J. *36*, 2726–2741.
29. Bjerregaard, V.A., Garribba, L., McMurray, C.T., Hickson, I.D., and Liu, Y. (2018). Folate deficiency drives mitotic missegregation of the human FRAXA locus. Proc. Natl. Acad. Sci. USA *115*, 13003–13008.
30. Yudkin, D., Hayward, B.E., Aladjem, M.I., Kumari, D., and Usdin, K. (2014). Chromosome fragility and the abnormal replication of the FMR1 locus in fragile X syndrome. Hum. Mol. Genet. *23*, 2940–2952.
31. Garribba, L., Bjerregaard, V.A., Gonçalves Dinis, M.M., Özer, Ö., Wu, W., Sakellariou, D., Pena-Diaz, J., Hickson, I.D., and Liu, Y. (2020). Folate stress induces SLX1- and RAD51-dependent mitotic DNA synthesis at the fragile X locus in human cells. Proc. Natl. Acad. Sci. USA *117*, 16527–16536.
32. Kockler, Z.W., Osia, B., Lee, R., Musmaker, K., and Malkova, A. (2021). Repair of DNA Breaks by Break-Induced Replication. Annu. Rev. Biochem. *90*, 165–191.
33. Botuyan, M.V., Lee, J., Ward, I.M., Kim, J.E., Thompson, J.R., Chen, J., and Mer, G. (2006). Structural basis for the methylation state-specific recognition of histone H4-K20 by 53BP1 and Crb2 in DNA repair. Cell *127*, 1361–1373.
34. Pellegrino, S., Michelena, J., Teloni, F., Imhof, R., and Altmeyer, M. (2017). Replication-Coupled Dilution of H4K20me2 Guides 53BP1 to Pre-replicative Chromatin. Cell Rep. *19*, 1819–1831.
35. Svobodová Kovaříková, A., Legartová, S., Krejčí, J., and Bártová, E. (2018). H3K9me3 and H4K20me3 represent the epigenetic landscape for 53BP1 binding to DNA lesions. Aging (Albany NY) *10*, 2585–2605.
36. Srivastava, M., Nambiar, M., Sharma, S., Karki, S.S., Goldsmith, G., Hegde, M., Kumar, S., Pandey, M., Singh, R.K., Ray, P., et al. (2012). An inhibitor of nonhomologous end-joining abrogates double-strand break repair and impedes cancer progression. Cell *151*, 1474–1487.
37. Huang, F., Motlekar, N.A., Burgwin, C.M., Napper, A.D., Diamond, S.L., and Mazin, A.V. (2011). Identification of specific inhibitors of human RAD51 recombinase using high-throughput screening. ACS Chem. Biol. *6*, 628–635.
38. Alagpulinsa, D.A., Ayyadevara, S., and Shmookler Reis, R.J. (2014). A Small-Molecule Inhibitor of RAD51 Reduces Homologous Recombination and Sensitizes Multiple Myeloma Cells to Doxorubicin. Front. Oncol. *4*, 289.
39. Huang, F., and Mazin, A.V. (2014). A small molecule inhibitor of human RAD51 potentiates breast cancer cell killing by therapeutic agents in mouse xenografts. PLoS One *9*, e100993.
40. Schotta, G., Lachner, M., Sarma, K., Ebert, A., Sengupta, R., Reuter, G., Reinberg, D., and Jenuwein, T. (2004). A silencing pathway to induce H3-K9 and H4-K20 trimethylation at constitutive heterochromatin. Genes Dev. *18*, 1251–1262.
41. Usdin, K., and Woodford, K.J. (1995). CGG repeats associated with DNA instability and chromosome fragility form structures that block DNA synthesis in vitro. Nucleic Acids Res. *23*, 4202–4209.
42. Fry, M., and Loeb, L.A. (1994). The fragile X syndrome d(CGG)n nucleotide repeats form a stable tetrahelical structure. Proc. Natl. Acad. Sci. USA *91*, 4950–4954.
43. Gacy, A.M., Goellner, G., Juranić, N., Macura, S., and McMurray, C.T. (1995). Trinucleotide repeats that expand in human disease form hairpin structures in vitro. Cell *81*, 533–540.
44. Mitas, M., Yu, A., Dill, J., and Haworth, I.S. (1995). The trinucleotide repeat sequence d(CGG)15 forms a heat-stable hairpin containing Gsyn. Ganti base pairs. Biochemistry *34*, 12803–12811.
45. Yu, A., Barron, M.D., Romero, R.M., Christy, M., Gold, B., Dai, J., Gray, D.M., Haworth, I.S.,

and Mitas, M. (1997). At physiological pH, d(CCG)15 forms a hairpin containing protonated cytosines and a distorted helix. Biochemistry *36*, 3687–3699.

46. Kettani, A., Kumar, R.A., and Patel, D.J. (1995). Solution structure of a DNA quadruplex containing the fragile X syndrome triplet repeat. J. Mol. Biol. *254*, 638–656.
47. Kamath-Loeb, A.S., Loeb, L.A., Johansson, E., Burgers, P.M., and Fry, M. (2001). Interactions between the Werner syndrome helicase and DNA polymerase delta specifically facilitate copying of tetraplex and hairpin structures of the d(CGG)n trinucleotide repeat sequence. J. Biol. Chem. *276*, 16439–16446.
48. Murat, P., Guilbaud, G., and Sale, J.E. (2020). DNA polymerase stalling at structured DNA constrains the expansion of short tandem repeats. Genome Biol. *21*, 209.
49. Casas-Delucchi, C.S., Daza-Martin, M., Williams, S.L., and Coster, G. (2022). The mechanism of replication stalling and recovery within repetitive DNA. Nat. Commun. *13*, 3953.
50. Gerhardt, J., Tomishima, M.J., Zaninovic, N., Colak, D., Yan, Z., Zhan, Q., Rosenwaks, Z., Jaffrey, S.R., and Schildkraut, C.L. (2014). The DNA replication program is altered at the FMR1 locus in fragile X embryonic stem cells. Mol. Cell *53*, 19–31.
51. Nolin, S.L., Glicksman, A., Houck, G.E., Jr., Brown, W.T., and Dobkin, C.S. (1994). Mosaicism in fragile X affected males. Am. J. Med. Genet. *51*, 509–512.
52. Dobkin, C., Radu, G., Ding, X.H., Brown, W.T., and Nolin, S.L. (2009). Fragile X prenatal analyses show full mutation females at high risk for mosaic Turner syndrome: fragile X leads to chromosome loss. Am. J. Med. Genet. *149A*, 2152–2157.
53. Coffee, B., Ikeda, M., Budimirovic, D.B., Hjelm, L.N., Kaufmann, W.E., and Warren, S.T. (2008). Mosaic FMR1 deletion causes fragile X syndrome and can lead to molecular misdiagnosis: a case report and review of the literature. Am. J. Med. Genet. *146A*, 1358–1367.
54. Gonçalves, T.F., dos Santos, J.M., Gonçalves, A.P., Tassone, F., Mendoza-Morales, G., Ribeiro, M.G., Kahn, E., Boy, R., Pimentel, M.M.G., and Santos-Rebouças, C.B. (2016). Finding FMR1 mosaicism in Fragile X syndrome. Expert Rev. Mol. Diagn. *16*, 501–507.
55. Tekendo-Ngongang, C., Grochowsky, A., Solomon, B.D., and Yano, S.T. (2021). Beyond Trinucleotide Repeat Expansion in Fragile X Syndrome: Rare Coding and Noncoding Variants in FMR1 and Associated Phenotypes. Genes *12*, 1669.
56. Verdyck, P., Berckmoes, V., De Vos, A., Verpoest, W., Liebaers, I., Bonduelle, M., and De Rycke, M. (2015). Chromosome fragility at FRAXA in human cleavage stage embryos at risk for fragile X syndrome. Am. J. Med. Genet. *167A*, 2306–2313.
57. Groh, M., Lufino, M.M.P., Wade-Martins, R., and Gromak, N. (2014). R-loops associated with triplet repeat expansions promote gene silencing in Friedreich ataxia and fragile X syndrome. PLoS Genet. *10*, e1004318.
58. Loomis, E.W., Sanz, L.A., Chédin, F., and Hagerman, P.J. (2014). Transcription-associated R-loop formation across the human FMR1 CGG-repeat region. PLoS Genet. *10*, e1004294.
59. Nikolov, I., and Taddei, A. (2016). Linking replication stress with heterochromatin formation. Chromosoma *125*, 523–533.
60. Dubarry, M., Loïodice, I., Chen, C.L., Thermes, C., and Taddei, A. (2011). Tight protein-DNA interactions favor gene silencing. Genes Dev. *25*, 1365–1370.
61. Lee, H.G., Imaichi, S., Kraeutler, E., Aguilar, R., Lee, Y.W., Sheridan, S.D., and Lee, J.T. (2023). Site-specific R-loops induce CGG repeat contraction and fragile X gene reactivation. Cell *186*, 2593–2609.e18.
62. Wöhrle, D., Salat, U., Hameister, H., Vogel, W., and Steinbach, P. (2001). Demethylation, reactivation, and destabilization of human fragile X full-mutation alleles in mouse embryocarcinoma cells. Am. J. Hum. Genet. *69*, 504–515.
63. Hayward, B.E., Zhou, Y., Kumari, D., and Usdin, K. (2016). A Set of Assays for the Comprehensive Analysis of FMR1 Alleles in the Fragile X-Related Disorders. J. Mol. Diagn. *18*, 762–774.
64. Taylor, A.K., Tassone, F., Dyer, P.N., Hersch, S.M., Harris, J.B., Greenough, W.T., and Hagerman, R.J. (1999). Tissue heterogeneity of the FMR1 mutation in a high-functioning male with fragile X syndrome. Am. J. Med. Genet. *84*, 233–239.
65. Kumari, D., Hayward, B., Nakamura, A.J., Bonner, W.M., and Usdin, K. (2015). Evidence for chromosome fragility at the frataxin locus in Friedreich ataxia. Mutat. Res. *781*, 14–21.
66. Krasilnikova, M.M., and Mirkin, S.M. (2004). Replication stalling at Friedreich's ataxia (GAA)n repeats in vivo. Mol. Cell Biol. *24*, 2286–2295.
67. Kumari, D., and Usdin, K. (2014). Polycomb group complexes are recruited to reactivated FMR1 alleles in Fragile X syndrome in response to FMR1 transcription. Hum. Mol. Genet. *23*, 6575–6583.

STAR★METHODS

KEY RESOURCES TABLE

REAGENT or RESOURCE	SOURCE	IDENTIFIER
Antibodies		
Anti-histone H4 trimethyl K20	Active motif	RRID: AB_2650526
HRP-labeled secondary anti-mouse IgG antibody	GE Healthcare Bio-Sciences	RRID: AB_772210
anti-histone H4	Abcam	RRID: AB_296888
HRP-labeled secondary anti-rabbit IgG antibody	GE Healthcare Bio-Sciences	RRID_772206
anti-histone H4 dimethyl K20	Diagenode	RRID: AB_2877177
anti-histone H4 trimethyl K20	Abcam	RRID: AB_306969
Anti-53BP1	Novus Biologicals	RRID: AB_10001695
Normal Rabbit IgG	EMD-Millipore	Cat# 12-270
Chemicals, peptides, and recombinant proteins		
Colcemid	Roche/Sigma-Aldrich	Cat# 10295892001
SEEBRIGHT® Orange 552 dUTP	Enzo Life Sciences	Cat# ENZ-42842
Pepsin	Roche/Sigma-Aldrich	Cat# 10108057001
Decitabine (5-azadeoxycytidine)	Cayman Chemical Company	Cat# 11166
A-196 (6,7-dichloro-N-cyclopentyl-4-(4-pyridinyl)-1-phthalazinamine)	Tocris	Cat# 6167
SCR7	Selleckchem	Cat# S7742
B02	Selleckchem	Cat# S8434
5-Fluoro-2′-deoxyuridine	Sigma-Aldrich	Cat# F0503
Dimethyl sulfoxide	Sigma-Aldrich	Cat# D2650
Critical commercial assays		
SuperScript™ IV VILO™ master mix	Thermo Fisher Scientific	Cat# 11756500
TaqMan™ Fast Advanced master mix	Thermo Fisher Scientific	Cat# 4444964
Human FMR1 (FAM-MGB) TaqMan™ assay	Thermo Fisher Scientific	Assay ID Hs00924547_m1
Human GUSB (Beta Glucuronidase) Endogenous Control (VIC™/MGB probe, primer limited)	Thermo Fisher Scientific	Cat# 4326320E
TRIzol™ Reagent	Thermo Fisher Scientific	Cat# 15596018
Power SYBR™ Green PCR master mix	Thermo Fisher Scientific	Cat# 4368702
Nick translation kit	Roche	Cat# 10976776001
Trans-Blot Turbo RTA mini 0.2 µm nitrocellulose transfer kit	Bio-Rad Laboratories	Cat# 1704270
4-20% EXpressPlus™ PAGE gel	GenScript	Cat# M42012
Experimental models: Cell lines		
GM06865	Coriell Cell Repositories	RRID: CVCL_N056
GM06895	Coriell Cell Repositories	RRID: CVCL_F299
GM06892	Coriell Cell Repositories	RRID: CVCL_AX90
GM06906	Coriell Cell Repositories	RRID: CVCL_AX97
GM04025	Coriell Cell Repositories	RRID: CVCL_1N28
GM07294	Coriell Cell Repositories	RRID: CVCL_AY12
Oligonucleotides		
FMR1 Exon1-F	Invitrogen	5′-CGCTAGCAGGGCTGAAGAGAA-3′
FMR1 Exon1-R	Invitrogen	5′-GTACCTTGTAGAAAGCGCCATTGGAG-3′
hs*GAPDH* exon 1F1	Invitrogen	5′-TCGACAGTCAGCCGCATCT-3′
hs*GAPDH* intron1 R1	Invitrogen	5′-CTAGCCTCCCGGGTTTCTCT-3′

(*Continued on next page*)

Continued

REAGENT or RESOURCE	SOURCE	IDENTIFIER
Recombinant DNA		
BAC clone for FMR1 FISH (GenBank: AC233288.1)	BACPAC Resources Center, Children's Hospital Oakland Research Institute. https://bacpacresources.org	RP11-383P16
Software and algorithms		
AlphaView	Proteinsimple	N/A
Student's *t* test	GraphPad Software	https://www.graphpad.com/quickcalcs/
Fisher's exact test	GraphPad Software	https://www.graphpad.com/quickcalcs/

RESOURCE AVAILABILITY

Lead contact

Further information and requests for resources and reagents should be directed to, and will be fulfilled by, the lead contact, Dr. Karen Usdin (karenu@nih.gov).

Materials availability

This study did not generate new unique reagents.

Data and code availability

- All data generated in this study is available in the main text and as supplemental information.
- This paper does not report original code.
- Any additional information required to reanalyze the data reported in this paper is available from the lead contact upon request.

EXPERIMENTAL MODEL AND STUDY PARTICIPANT DETAILS

Human cell lines

Lymphoblastoid cell lines derived from healthy controls/typical (GM06865 [30 CGG, RRID:CVCL_N056], GM06895 [23 CGG, RRID:CVCL_F299]), individuals carrying premutation alleles (GM06906 [96 CGG, RRID:CVCL_AX97], GM06892 [93 CGG, RRID:CVCL_AX90]) and fragile X syndrome (FXS) patients (GM04025 [645 CGG, RRID:CVCL_1N28], GM07294 [745 CGG, RRID:CVCL_AY12]) were obtained from Coriell Cell Repositories (Coriell Institute for Medical Research, Camden, NJ). All cell lines used in this study were derived from male individuals. The CGG repeat size and methylation status was confirmed by PCR as previously described.[63]

METHOD DETAILS

Cell culture and drug treatments

The lymphoblastoid cells were grown in Roswell Park Memorial Institute (RPMI) 1640 medium supplemented with 10% fetal bovine serum (FBS) and 1X antibiotic-antimycotic (all from Thermo Fisher Scientific, Waltham, MA). The compound A-196 (6,7-dichloro-N-cyclopentyl-4-(4-pyridinyl)-1-phthalazinamine) was obtained from the Structural Genomics Consortium (Toronto, ON, Canada) for initial studies and later from Tocris (Minneapolis, MN, # 6167). It was dissolved in Dimethyl sulfoxide (DMSO) to make a 5 mM stock solution and used at a final concentration of 5 μM and 10 μM. Decitabine (5-azadeoxycytidine, AZA) was purchased from Cayman Chemical Company (Ann Arbor, MI, # 11166) and dissolved in DMSO to make a 10 mM stock solution and used at 10 μM final concentration. For *FMR1* reactivation studies, FXS cells were treated with 5 μM A-196 for 3 days and collected for RNA isolation. For drug combination studies, FXS cells were treated with 10 μM AZA for 3 days and then split into two for treatment with either DMSO or 5 μM A-196 and grown for 24 days. The medium was changed, and fresh drugs added every 7 days and cells were collected for RNA at indicated time points. 5-Fluoro-2′-deoxyuridine (FdU) was obtained from Sigma-Aldrich (St. Louis, MO, #F0503) and a 100 μM stock solution was prepared in DMSO. The NHEJ inhibitor, SCR7 (catalog #S7742), and the RAD51 inhibitor, B02 (#S8434) were obtained from Selleckchem (Houston, TX) and a 10 mM stock solution was prepared in DMSO for each. For fluorescent *in situ* hybridization (FISH) experiments, the cells were treated with 0.1 μM FdU for 18h and with 5 μM A-196 or 10 μM SCR7 for 3 days. For A-196 + FdU treatment, cells were treated with 5 μM A-196 for 3 days and 0.1 μM FdU was added for the last 18h of the treatment. For A-196 + B02 treatment, cells were treated with 5 μM A-196 and 10 μM B02 for 3 days.

RNA methods

Total RNA was isolated from cells using TRIzol reagent (Thermo Fisher Scientific, Waltham, MA) and quantified on DS-11 Spectrophotometer (DeNovix, Wilmington, DE). Three hundred nanograms of total RNA was reverse transcribed in 20 μL final volume using SuperScript IV VILO master mix (Thermo Fisher Scientific) as per manufacturer's instructions. Real-time PCR was performed in triplicate using 2 μL of the cDNA, FAM-labeled *FMR1* (Hs00924547_m1) and VIC-labeled *β-glucoronidase* (*GUSB*) endogenous control (# 4326320E) Taqman probe-primers (Thermo Fisher Scientific) and TaqMan Fast Advanced master mix (Thermo Fisher Scientific) on StepOnePlus Real-Time PCR system (Thermo Fisher Scientific). For quantitation, the comparative threshold (Ct) method was used.

Western blotting

To prepare total cell lysates, cells were pelleted at 250 × g for 6 min and washed once with ice-cold PBS supplemented with 1X protease inhibitor cocktail (Sigma-Aldrich, St. Louis, MO, #P8340) and 1X phosphatase inhibitor (Sigma-Aldrich, #P5726). The cell pellet was then re-suspended in the lysis buffer (10 mM Tris Cl pH 7.5, 1 mM EDTA pH 8.0, 1% Triton X-100, 1X protease inhibitor cocktail and 1X phosphatase inhibitor) and incubated on ice for 10 min followed by sonication for 30 s at medium setting using Bioruptor (Diagenode, Denville, NJ) to solubilize proteins and shear the DNA. The protein amount was quantified using Bio-Rad Protein Assay Dye Reagent Concentrate (Bio-Rad Laboratories, Inc., Hercules, CA, #5000006) as per manufacturer's protocol. Before using the lysate for Western blot analyses, 1X volumes of Novex LDS Sample Buffer (Thermo Fisher Scientific, catalog #NP0007) and NuPAGE Sample Reducing Agent (Thermo Fisher Scientific, #NP0009) were added, and the samples were heated at 75°C for 10 min. Ten micrograms of total cell lysates were run on a 4–20% EXpressPlus PAGE gel (GenScript, Piscataway, NJ, #M42012) in Tris-MOPS-SDS running buffer (GenScript, #M00138) for 40 min at 120 V and transferred to nitrocellulose membrane using the Trans-Blot Turbo RTA mini 0.2 μm nitrocellulose transfer kit (#1704270) and Trans-Blot Turbo Transfer system from Bio-Rad Laboratories. The membrane was blocked for 2 h with 5% blocking agent (GE Healthcare Bio-Sciences, Pittsburg, PA, #RPN2125) in TBST (1X Tris-buffered saline with 0.1% Tween 20). The blot was incubated with 1:2000 dilution of antibody against histone H4 trimethyl K20 (Active motif, Carlsbad, CA, #39671, RRID:AB_2650526) overnight at 4°C, washed three times with TBST for 5 min each and then probed with 1:5000 diluted HRP-labeled secondary anti-mouse IgG antibody (GE Healthcare Bio-Sciences, #NA931, RRID:AB_772210) for 1 h. The blot was then washed three times with TBST for 5 min each and once with TBS. The signal was detected using ECL Prime detection reagents (GE Healthcare Bio-Sciences) and imaged with Fluorchem M imaging system (Proteinsimple, Santa Clara, CA). The blot was then stripped with Restore Western Blot stripping buffer (Thermo Fisher Scientific, catalog #21059) and re-probed with 1:5000 dilution of anti-histone H4 (Abcam, Cambridge, MA, #ab10158, RRID:AB_296888) overnight at 4°C, washed three times with TBST for 5 min each and then probed with 1:5000 diluted HRP-labeled secondary anti-rabbit IgG antibody (GE Healthcare Bio-Sciences, #NA934, RRID_772206) for 1 h. The blot was then washed three times with TBST for 5 min each and once with TBS. The signal was detected using ECL Prime detection reagents (GE Healthcare Bio-Sciences) and imaged with Fluorchem M imaging system (Proteinsimple, Santa Clara, CA). The quantification was done using the AlphaView software for FluorChem Systems (Proteinsimple) and the amounts of methylated histones were normalized to the amount of total H4.

Chromatin immunoprecipitation

Chromatin immunoprecipitation (ChIP) assays for histone modifications were performed as described before[67] using a ChIP assay kit from EMD-Millipore (Billerica, MA). To prepare chromatin for immunoprecipitation, cells were fixed with 1% formaldehyde for 10 min at room temperature and lysed as per the kit manufacturer's instructions. The chromatin was sonicated into <500 bp fragments using a Bioruptor (Diagenode) for 6 min with 30 s ON and 30 s OFF at medium setting. Twenty micrograms of chromatin were used in each immunoprecipitation reaction with 5 μg each of normal Rabbit IgG (EMD-Millipore, # 12–270), anti-histone H4 trimethyl K20 (Abcam, # ab9053, RRID:AB_306969), anti-histone H4 dimethyl K20 (Diagenode Inc., Denville, NJ; #C15200205, RRID:AB_2877177) and 53BP1 (Novus Biologicals, Centennial, CO; # NB100-305, RRID:AB_10001695). Slight modifications to the protocol were made for 53BP1 ChIP. Briefly, 30 μg of chromatin was used in each ChIP reaction and modified wash steps were used: 1× with low salt wash buffer from the ChIP assay Kit (Millipore) for 5 min, 1× with wash buffer II (50 mm HEPES-KOH, pH 7.5, 500 mm NaCl, 1 mm EDTA pH 8.0, 1% Triton X-100, 0.1% sodium deoxycholate) for 5 min, 1× with wash buffer III (10 mm Tris, pH 8.0, 250 mm LiCl, 1 mm EDTA, pH 8.0, 0.5% IGEPAL-CA630, 0.5% sodium deoxycholate) for 5 min followed by two washes with Tris-EDTA, pH 8.0, for 5 min each. Real-time PCRs on the immunoprecipitated DNAs were carried out in triplicate in 20 μL final volume using the Power SYBR Green PCR master mix (Thermo Fisher Scientific, # 4368702) and 200 nM of each primer and 2 μL of DNA. For amplification of *FMR1* exon 1, the primer pair Exon 1-F (5′-CGCTAGCAGGGCTGAAGAGAA-3′) and Exon1-R (5′-GTACCTTG TAGAAAGCGCCATTGGAG-3′) was used. This primer pair amplifies the region +236 to +312 relative to the transcription start site. For the amplification of a control active genomic locus, GAPDH (accession number BC025925), primers hs*GAPDH* exon 1 F1 (5′-TCGACAGT CAGCCGCATCT-3′) and hs*GAPDH* intron1 R1 (5′-CTAGCCTCCCGGGTTTCTCT-3′) were used. For quantitation, the comparative threshold (Ct) method was used. Enrichment in ChIP samples was calculated over 100% of input and normalized to vehicle (DMSO) treated samples.

Fluorescent *in situ* hybridization (FISH)

To prepare metaphase chromosomes for FISH analysis, cells were incubated with colcemid (0.1 g/mL) for 3 h before being harvested. The cell pellet was carefully resuspended in 5 mL of pre-warmed (37°C) 75 mM KCl (Sigma, St Louis, MO). The cell suspension was then incubated for 25 min at 37°C. Cells were subsequently centrifuged for 5 min (300 × g) and resuspended with 5 mL of fixation solution (methanol: acetic acid,

3:1). This step was subsequently performed two more times before the cells were dropped onto glass slides inside an environmental control chamber (Thermotron, Holland, MI). The FISH probe for FRAXA was prepared using the BAC clone: RP11-383P16 (GenBank: AC233288.1), which was directly labeled in Orange-dUTP (Enzo, New York, NY) using nick-translation (Roche, Indianapolis, IN). For FISH, the slides were equilibrated in 2X SSC for 5 min at RT, treated with 3μL of pepsin (100 mg/mL) dissolved in 100 mL of pre-warmed (37°C) 0.01 M HCl for 5 min followed by dehydration in an ethanol series (70%, 90%, 100%) at room temperature for 3 min each. The slides were then treated with 70% formamide at 72°C for 15 s and dehydrated again in an ice-cold ethanol series (70%, 90%, 100%) for 3 min each. FISH-probe hybridization was carried out overnight at 37°C for at least 16h. Slides were imaged using an automated metaphase finder program on the DUET scanning imaging workstation (BioView Ltd., Rehovot, Israel, software version 3.6.0.15). All signals were manually counted and reviewed for accuracy using the SOLO workstation (BioView Ltd.). On average, 100 metaphases were evaluated per treatment condition.

QUANTIFICATION AND STATISTICAL ANALYSIS

Statistical significance of observed differences was calculated using paired two-tailed Student's *t* test and/or Fisher's exact test (GraphPad Software, Inc., La Jolla, CA), and a p value of ≤ 0.05 was considered statistically significant. Specific details can be found in the results and the figure legends.